Coupled chirped vertical gratings for on-chip group velocity dispersion engineering

D. T. H. Tan,[a] K. Ikeda, and Y. Fainman
Department of Electrical and Computer Engineering, University of California San Diego, 9500 Gilman Drive, La Jolla, California 92093-0409, USA

(Received 24 August 2009; accepted 11 September 2009; published online 8 October 2009)

Coupled chirped vertical gratings are proposed for on-chip group velocity dispersion engineering. The device circumvents the need for directional couplers or circulators to redirect compensated data. Finite difference time domain simulations and experimental verification of fabricated devices are performed. Dispersion values of up to 8.4×10^5 ps/nm/km are demonstrated. © *2009 American Institute of Physics*. [doi:10.1063/1.3242028]

As the need for faster data transmission rates and wider bandwidths makes its way into mainstream telecommunications, new methods to overcome some of the inherent issues in utilizing silicon on insulator (SOI) as a material platform will need to be resolved. One such problem is potential data loss from group velocity dispersion (GVD) induced pulse broadening. In SOI waveguides, the high waveguide contribution to the GVD leads to dispersion two orders of magnitude larger than that of silica fibers.[1,2] In this letter, we aim to solve this issue by developing an on-chip GVD compensator to preserve the integrity of transmitted data. The method involves using two coupled chirped vertical Bragg gratings (CBGs) to simultaneously compensate for GVD and reroute the compensated data without any concomitant loss. We have previously demonstrated a single chirped grating for GVD engineering[3] on SOI. However, the lack of a viable on-chip circulator implies either a 6 dB loss from rerouting the data through directional couplers, or heterogeneous integration with a fiber based circulator. Here we present a device geometry that allows for conceptually lossless operation, and demonstrate GVD values of up to 8.4×10^5 ps/nm/km. It is evident that the ability to efficiently compensate for GVD will become increasingly important as silicon photonics gradually shifts from niche development to the mainstream.

A schematic diagram of the proposed device is shown in Fig. 1. The device is implemented using an SOI wafer with a 250 nm thick silicon layer on a 3 μm thick layer of buried oxide on a silicon substrate. Two channel waveguides with CBGs[3–5] are placed side by side such that we have three Bragg matching conditions.[6] The first two Bragg conditions satisfy coupling of the forward and backward propagating modes for each of the individual waveguide gratings and are of less interest. The third Bragg matching condition arises from the cross coupling between these two waveguide gratings. This condition may be described using the following coupled mode theory (CMT) equations:[6–8]

$$\frac{\partial A_1(z)}{\partial z} = -i\frac{\beta_1(\lambda)}{|\beta_1(\lambda)|}\kappa(z)A_2(z)e^{i\Delta\beta(\lambda)z},$$

$$\frac{\partial A_2(z)}{\partial z} = -i\frac{\beta_2(\lambda)}{|\beta_2(\lambda)|}\kappa^*(z)A_1(z)e^{-i\Delta\beta(\lambda)z},$$

where $A_1(z)$ and $A_2(z)$ represent the complex amplitudes of the forward mode in the input waveguide and the backward propagating mode in the output waveguide; the coupling coefficient, $\kappa(z)$ is defined as $\kappa(z)=\kappa_o f(z)e^{j\phi(z)}$ where κ_o is the maximum value of the coupling coefficient and $f(z)$ is the grating apodization function. The phase function, $\phi(z)=(\Delta\Lambda\cdot\pi\cdot z^2)/(\Lambda_0^2\cdot L)$ where $\Delta\Lambda$ is the total chirp in the grating period, Λ_o is the average CBG period, and L is the device length.[7] The Bragg detuning, $\Delta\beta(\lambda)=\beta_1(\lambda)-\beta_2(\lambda)-2\pi/\Lambda_o$ where $\beta_{1,2}(\lambda)$ are the propagation constants for the forward mode in waveguide 1 and the backward mode in waveguide 2, respectively. The period of individual CBGs at any point, z is given by $\Lambda(z)=\Lambda_0+\Delta\Lambda.z/L$. In the case of the coupled gratings, the coupling strength is determined by the gap width G and the modulation amplitudes $\Delta W_{1,2}$ of gratings 1 and 2, respectively. The relationship between coupling strength between the two waveguides, κ_o and G has been calculated in Ref. 9. We set values for ΔW_1 at 50 nm, ΔW_2 at 30 nm, and Λ_o at 305 nm to ensure that the Bragg detuning is zero at 1.55 μm. Due to the current limitation in the device lengths that we can fabricate without stitching in our electron-beam (e-beam) lithography system, we limit L to 100 μm. Consequently, to ensure transmission of close to 100%, we set G at 80 nm. The small value of G results in a large coupling strength (~285/cm) (Ref. 9) and thus for better accuracy over CMT, we perform two-dimensional (2D) finite difference time domain (FDTD) simulations, with a 5 $\times10$ nm^2 grid size, to analyze the device. The modeling

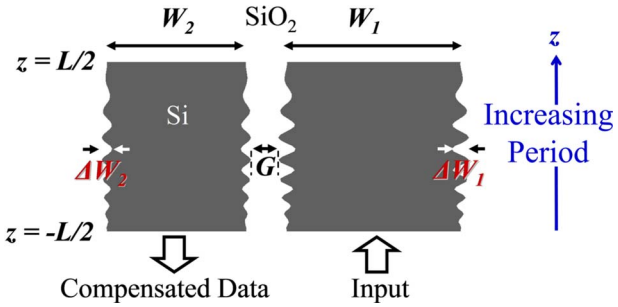

FIG. 1. (Color online) Schematic diagram of coupled CBG device. $W_1=500$ nm, $W_2=400$ nm, $\Delta W_1=50$ nm, and $\Delta W_2=30$ nm.

[a]Electronic mail: thtan@ucsd.edu.

results are approximate because of the reduction of the three-dimensional problem to a 2D one. The effective index of the silicon slab of height 250 nm, infinite in the horizontal direction is used in place of the material refractive index of silicon. Symmetric Blackman apodization is applied to suppress group delay ripple in the spectra.[5,10] The modeled transmission and group delay characteristics for devices with $\Delta\Lambda = 4$ and 7 nm are shown in Figs. 2(a) and 2(b). We observe that the group delay characteristics are relatively linear within the passbands, with minimal group delay ripple. The corresponding average values of GVD within the two passbands are 0.078 and 0.039 ps/nm and the resultant transmission bandwidths are 25 and 37 nm.

The transmission of the gratings is lower than 100% and decreases for larger $\Delta\Lambda$ owing to the lower effective coupling for each wavelength component. Transmission close to 100% may be achieved for longer device lengths. The out of band sidelobe observed at 1.5 μm in Fig. 2(a) is a result of small G. Since gratings 1 and 2 behave as waveguides outside of the main transmission band, coupling of copropagating modes between the adjacent waveguides can occur. Some light couples from the right grating into the left grating, and undergoes a reflection under the left grating's Bragg condition, $2\beta_2 = 2\pi/\Lambda_0$ centered at 1.5 μm, resulting in a small out of band sidelobe [Fig. 2(a)]. The unwanted coupling may be eliminated by increasing G since the maximum power transfer varies inversely with κ_o for $\beta_1 \neq \beta_2$. Since the bandwidth is a function of both $\Delta\Lambda$ and κ, $\Delta\Lambda$ may then be increased to achieve the same bandwidth. Additionally, the sign of the dispersion may be changed by inverting the direction of the chirp in order to generate either normal or anomalous GVD. Applications requiring larger bandwidth may be accommodated for by increasing $\Delta\Lambda$.

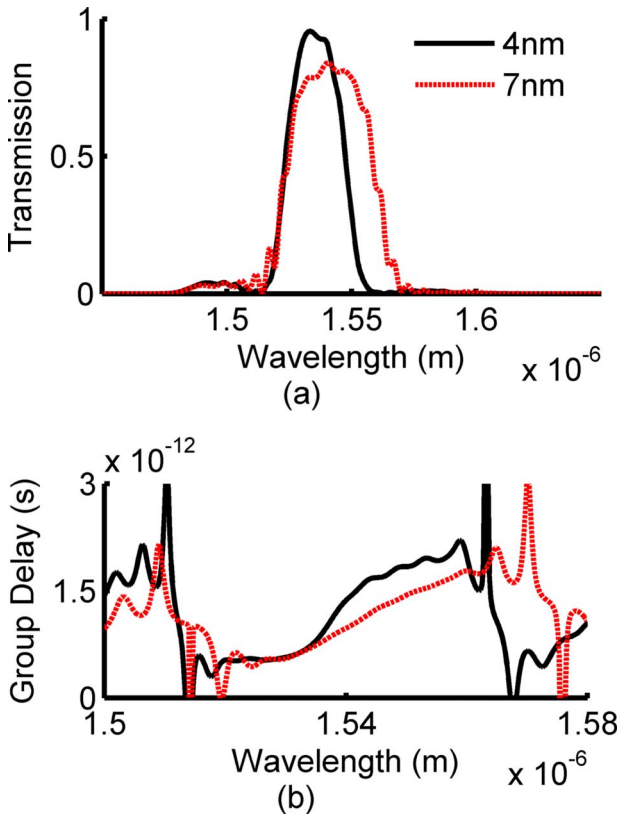

FIG. 2. (Color online) (a) Transmission spectra and (b) group delay of coupled CBG device for $G=80$ nm, $L=100$ μm, $\Delta\Lambda=4$ nm (solid black line), and 7 nm (dotted red line) calculated using 2D FDTD.

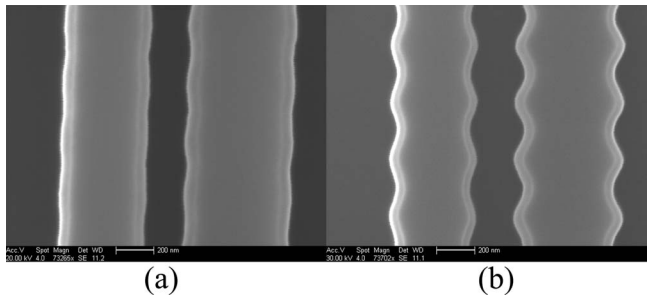

FIG. 3. SEM micrographs of fabricated coupled CBG devices. Apodization of the grating amplitude is shown at the (a) input and (b) center sections of the fabricated device.

The coupled CBGs were fabricated using e-beam lithography and reactive ion etching. A 2 μm thick SiO_2 overcladding layer is deposited over the device using plasma-enhanced chemical vapor deposition. Scanning electron micrographs (SEM) of fabricated devices are shown in Fig. 3. Experimental characterization of the fabricated devices was performed using a technique similar to that used in Refs. 3 and 10. The cleaved facet of the input waveguide and the start of the device form mirrors which result in Fabry-Pérot (FP) oscillations with period, $\Delta\lambda$ in the transmission spectra. The resulting cavity length, l_c is a function of wavelength and is found using $l_c = \lambda^2/2n_g\Delta\lambda$. The group delay, τ as a function of wavelength is then given by $\tau = 2n_g l_c/c$. Assuming the group index, $n_g = 4.4$ (calculated using a fully vectorial beam propagation method for the left waveguide), we obtain the GVD using the slope of a linear fit to the extracted group delay. Figure 4(a) shows the transmission characteristics of fabricated devices for $\Delta\Lambda = 4$ and 7 nm showing the FP oscillations. The results clearly show the extension in bandwidth from 15 to 21 nm as $\Delta\Lambda$ increases from 4 to 7 nm. The bandwidth is lower than that expected from FDTD calculations. This is a result of the lower effective coupling coefficient obtained from G being slightly larger than 80 nm in the fabricated devices; SEM micrographs in Fig. 3(b)

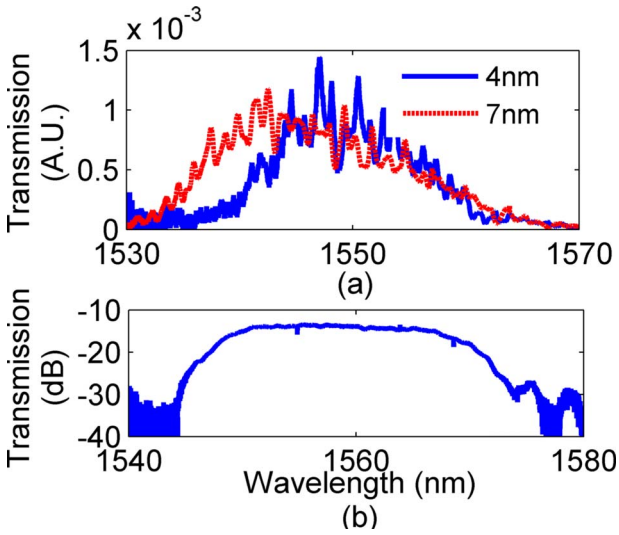

FIG. 4. (Color online) Measured transmission for (a) $\Delta\Lambda = 4$ nm (solid blue line) and 7 nm (dotted red line) showing FP oscillations, and (b) for $\Delta\Lambda = 4$ nm in the absence of FP oscillations.

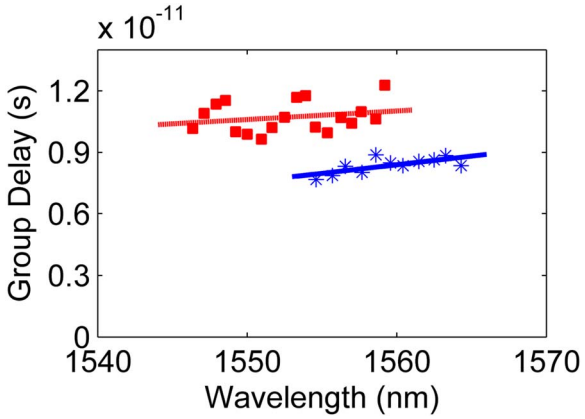

FIG. 5. (Color online) Measured group delay for $\Delta\Lambda=4$ nm (blue stars) and 7 nm (red squares) with linear fits to measured data.

show that G obtained is slightly larger than 80 nm. The relationship between G and κ is inversely exponential due to the evanescent decay of the fields from the grating.

The smaller achieved bandwidth implies that we expect a larger GVD value. This is attributed to the group delay being distributed over a smaller wavelength range. Indeed we observe slightly larger GVD values from those predicted by the modeling results. Figure 5 shows plots of the measured group delay and the linear fits to the measured experimental data. The GVD for $\Delta\Lambda=4$ and 7 nm are 0.084 and 0.042 ps/nm, respectively. For better characterization of the transmission characteristics, we terminate all ports with inverse tapers[11] to eliminate FP oscillations. Figure 4(b) shows the transmission of the fabricated device with $\Delta\Lambda=4$ nm and inverse tapers, demonstrating the flat top profile and effectiveness of the applied apodization in minimizing ripple.

In addition to GVD compensation, the presented device may also be useful for integrated photonics applications requiring dispersive elements. For example, two such gratings with chirp values equal in magnitude but opposite in sign may be used as matched dispersive elements for performing temporal Fourier transforms.[12,13] This eliminates the need for heterogeneous integration of fiber-based dispersive elements with integrated photonics circuits.

In conclusion, we propose a dispersive device implemented on SOI constructed with coupled CBGs for on-chip GVD engineering. The modeling and experimental results are found to be in good agreement. The demonstrated technique is effective for efficient engineering of normal or anomalous dispersion necessary for various applications. The technique does not require an on-chip circulator for lossless operation, resolving the issue of using lossy directional couplers for data rerouting.

This work was supported by the Defense Advanced Research Projects Agency, the National Science Foundation, the NSF CIAN ERC, and the U.S. Army Research Office.

[1] A. C. Turner, C. Manolatou, B. S. Schmidt, M. Lipson, M. A. Foster, J. E. Sharping, and A. L. Gaeta, Opt. Express **14**, 4357 (2006).
[2] E. Dulkeith, F. Xia, L. Schares, and M. J. William, Opt. Express **14**, 3853 (2006).
[3] D. T. H. Tan, K. Ikeda, R. E. Saperstein, B. Slutsky, and Y. Fainman, Opt. Lett. **33**, 3013 (2008).
[4] J. T. Hastings and H. Michael, J. Vac. Sci. Technol. B **20**, 2753 (2002).
[5] H.-C. Kim, K. Ikeda, and Y. Fainman, Opt. Lett. **32**, 539 (2007).
[6] A. Yariv and P. Yeh, *Optical Waves in Crystals: Propagation and Control of Laser Radiation* (Wiley, New York, 2002).
[7] H. Kogelnik, Bell Syst. Tech. J. **55**, 109 (1975).
[8] P. Yeh and H. F. Taylor, Appl. Opt. **19**, 2848 (1980).
[9] K. Ikeda, M. Nezhad, and Y. Fainman, Appl. Phys. Lett. **92**, 201111 (2008).
[10] M. Notomi, K. Yamada, A. Shinya, J. Takahashi, C. Takahashi, and I. Yokohama, Phys. Rev. Lett. **87**, 253902 (2001).
[11] V. R. Almeida, R. R. Panepucci, and M. Lipson, Opt. Lett. **28**, 1302 (2003).
[12] R. E. Saperstein and Y. Fainman, Appl. Opt. **47**, A21 (2008).
[13] M. A. Foster, R. Salem, D. F. Geraghty, A. C. Turner-Foster, M. Lipson, and A. L. Gaeta, Nature (London) **456**, 81 (2008).